

## Thermally activated dissipation in a novel foamed Bi-based oxide superconductor in magnetic fields

To cite this article: K A Shaykhtudinov *et al* 2007 *Supercond. Sci. Technol.* **20** 491

View the [article online](#) for updates and enhancements.

### Related content

- [Study of dependence upon the magnetic field and transport current of the magnetoresistive effect in YBCO-based bulk composites](#)  
D A Balaev, A G Prus, K A Shaykhtudinov *et al.*
- [Thermally activated dissipation and pinning mechanisms in a Bi2223 superconductor with the addition of nanosized ZrO<sub>2</sub> particles](#)  
M Zouaoui, L Bessais and M Ben Salem
- [Proximity effect and electron transport in oxide hybrid heterostructures with superconducting/magnetic interfaces](#)  
G A Ovsyannikov, K Y Constantinian, Yu V Kisilinski *et al.*

### Recent citations

- [Highly Porous Superconductors: Synthesis, Research, and Prospects](#)  
D. M. Gokhfeld *et al*
- [Impact of Dy<sub>2</sub>O<sub>3</sub> nanoparticles additions on the properties of porous YBCO ceramics](#)  
M. A. Almessiere *et al*
- [Dissipation in granular high-temperature superconductors: New approach to describing the magnetoresistance hysteresis and the resistive transition in external magnetic fields](#)  
S. V. Semenov *et al*



**IOP | ebooks™**

Bringing together innovative digital publishing with leading authors from the global scientific community.

Start exploring the collection—download the first chapter of every title for free.

# Thermally activated dissipation in a novel foamed Bi-based oxide superconductor in magnetic fields

K A Shaykhutdinov<sup>1</sup>, D A Balaev<sup>1</sup>, S I Popkov<sup>1</sup>, A D Vasilyev<sup>1</sup>,  
O N Martyanov<sup>2</sup> and M I Petrov<sup>1</sup>

<sup>1</sup> Kirensky Institute of Physics, Akademgorodok 50, 660036 Krasnoyarsk, Russia

<sup>2</sup> Borekov Institute of Catalysis, Lavrent'ev avenue 5, 630090 Novosibirsk, Russia

E-mail: [smp@iph.krasn.ru](mailto:smp@iph.krasn.ru) (Shaykhutdinov)

Received 26 January 2007, in final form 19 March 2007

Published 25 April 2007

Online at [stacks.iop.org/SUST/20/491](http://stacks.iop.org/SUST/20/491)

## Abstract

The transport properties of a novel foamed superconductor  $\text{Bi}_{1.8}\text{Pb}_{0.3}\text{Sr}_{1.9}\text{Ca}_2\text{Cu}_3\text{O}_x$  have been studied. As the analysis of resistive transitions in a magnetic field shows, the dissipation follows a thermally activated flux creep model with the temperature-independent pinning potential in S–N–S-type Josephson junctions.

## 1. Introduction

High-temperature superconductors with low density and porous microstructure are considered to be representatives of a new class of disordered superconducting materials with fractal dimensions exhibiting intriguing physical properties [1, 2]. In our previous work [3, 4], the effect of microstructure of the bulk polycrystalline  $\text{Bi}_{1.8}\text{Pb}_{0.3}\text{Sr}_{1.9}\text{Ca}_2\text{Cu}_3\text{O}_x$  (BPSCCO) with low density on their magnetic and transport properties was described. It was found that the diamagnetic moment of foamed BPSCCO is significantly larger (about 2.4 times) than that of a bulk polycrystalline sample [3]. In [4], current–voltage characteristics (CVCs) of the foamed  $\text{Bi}_{1.8}\text{Pb}_{0.3}\text{Sr}_{1.9}\text{Ca}_2\text{Cu}_3\text{O}_x$  with a density of  $2.26 \text{ g cm}^{-3}$  (38% of the theoretical bulk density) at 77 and 4.2 K were studied. It was shown that the CVCs are adequately explained by theory [5], considering the fractal cluster structure of intergrain boundaries between normal and superconducting phases. Besides, the porous structure of these materials facilitates heat exchange between HTSC crystallites and refrigerating media, thus preventing the formation of hotspots, which can result in the increase in the current-carrying capability [2]. The above-mentioned specific features make these materials promising candidates for practical application.

In the present work we have studied the resistive transitions in the porous  $\text{Bi}_{1.8}\text{Pb}_{0.3}\text{Sr}_{1.9}\text{Ca}_2\text{Cu}_3\text{O}_x$  with a density of  $1.55 \text{ g cm}^{-3}$  (26% of the theoretical bulk density) in external magnetic fields. Also, the temperature dependence of the critical transport current density has been determined.

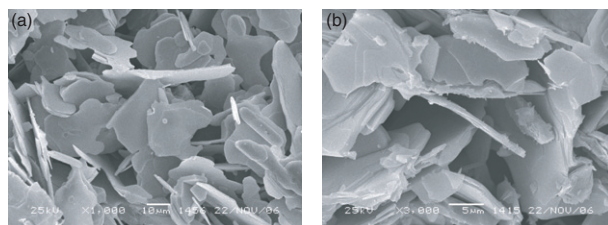


**Figure 1.** (a), (b) Scanning electron microscopy (SEM) images of  $\text{Bi}_{1.8}\text{Pb}_{0.3}\text{Sr}_{1.9}\text{Ca}_2\text{Cu}_3\text{O}_x$  (BPSCCO) with low density.

## 2. Experimental details

Samples of bulk polycrystalline  $\text{Bi}_{1.8}\text{Pb}_{0.3}\text{Sr}_{1.9}\text{Ca}_2\text{Cu}_3\text{O}_x$  (BPSCCO) with low density were prepared by the solid-state reaction technique; sintering time was 400 h [6]. The standard preparation method was used [7], except for the final heat treatment condition alteration that allowed us to obtain dominant growth of HTSC crystallites in the *ab* plane. Due to the random orientation of crystallites, this growth led to the material volume increase. Moreover, during the final heat treatment, the complete decomposition of calcium carbonate occurred. Carbonic gas overpressure during the process also resulted in the material volume increase. Scanning electron microscopy images (SEM) of a natural chip of the foamed BPSCCO are shown in figures 1(a) and (b). The density of the obtained material was  $1.55 \text{ g cm}^{-3}$  (26% of the theoretical one for the bulk BPSCCO). Due to the flatness of BPSCCO

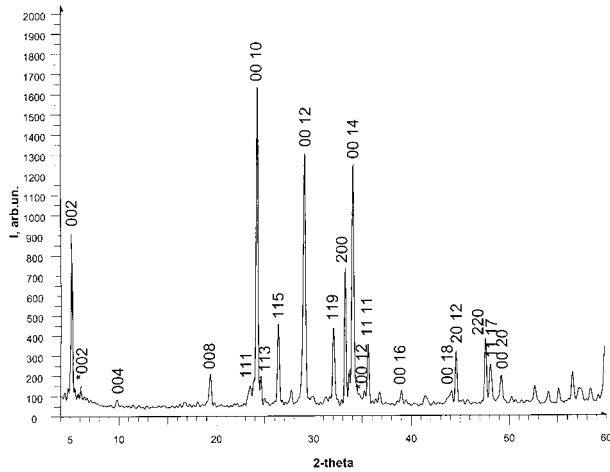


**Figure 2.** X-ray diffraction pattern of BPSCCO with low density.

crystallites, the superconducting foam has a pronounced flaky structure. As the SEM measurement results show, the foam consists of crystallites with the width 10–30  $\mu\text{m}$  and thickness 1–2  $\mu\text{m}$ . Between the crystallites, interstices are clearly seen.

An x-ray diffraction pattern of the foamed BPSCCO is presented in figure 2. It shows the reflections from Bi2223 and Bi2212 phases and their superposition. The phase ratio has been quantitatively evaluated using the (002) reflections. For the foamed BPSCCO,  $(I_{0022212}/I_{0022223}) \times 100\%$  is about 5%.

Current–voltage characteristics (CVCs) of the bulk polycrystalline  $\text{Bi}_{1.8}\text{Pb}_{0.3}\text{Sr}_{1.9}\text{Ca}_2\text{Cu}_3\text{O}_x$  (BPSCCO) with low density and temperature dependences of resistivity  $\rho(T)$  at different values of the applied magnetic field  $H$  were obtained by the standard four-probe technique at fixed current conditions; the cross section of the central part of the samples was  $\sim 1.5 \times 2 \text{ mm}^2$ ; the length of the samples was  $\sim 10 \text{ mm}$ . Values of the critical current  $J_c(T)$  were determined from the CVCs by a conventional criterion  $1 \mu\text{V cm}^{-1}$ . To avoid self-heating effects and improve heat exchange, the cell with a sample was immersed in a helium atmosphere. Superdispersed silver was burnt into the contact pads area, which made it possible to obtain contact resistance less than  $10^{-4} \Omega \text{ cm}^2$ . The applied field  $H$  was perpendicular to the transport current  $J$ .

### 3. Results and discussion

Above the superconducting transition, the  $R(T)$  dependence of the Bi-foamed superconductor is linear (see inset in figure 3). Extrapolation of a linear part of the  $R(T)$  dependence to  $T = 0$  gives the value  $R \approx 0$ . The resistive superconducting transition is sharp; the value of ‘zero-resistance’ critical temperature  $T_{C0}$  at  $H = 0$  is about 107 K (figure 3).

The effect of the magnetic field on the resistive superconducting transition is shown in figure 3. The external magnetic field broadens the resistive transition. In the presence of the magnetic field, the  $R(T)$  dependences are characterized by two distinctive sections; a steep part is associated with the superconductivity onset in crystallites and the broad foot structure. Such a behaviour is a remarkable feature of granular superconductors [8–11]. It is recognized that the mentioned

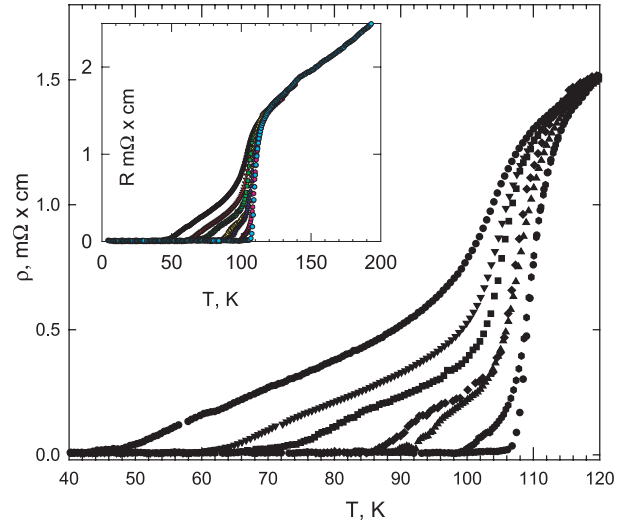


**Figure 3.**  $\rho(T, H)$  dependences of BPSCCO with low density. From right to left:  $H = 0, 0.1, 1, 2, 7, 20, 60 \text{ kOe}$ .

(This figure is in colour only in the electronic version)

broad-foot structure comes from the transition of intergrain boundaries, which are considered to be weak Josephson-type links. For this reason, let us consider processes taking place in a random network of Josephson junctions under the influence of a magnetic field. Some authors [8–10] interpreted the broadened part of  $R(T)$  dependences of the Bi-based polycrystalline superconductors in weak (hundreds Oe) magnetic fields by using the Ambegaokar–Halperin (AH) model of phase slip in Josephson junctions, or modifications of this model. We do not deny the possibility of a description of the experimental  $R(T)$  dependences of a Bi-foamed superconductor in magnetic fields below  $\sim 2 \text{ kOe}$  in the framework of the AH model. However, we have to note that large portions of the  $R(T)$  curves measured at  $H = 7, 20$  and  $60 \text{ kOe}$  are close to linear dependences (figure 3). This behaviour cannot be adequately explained by the AH theory. Similar features of the  $R(T)$  curves were reported for the polycrystalline  $\text{Bi}_{1.7}\text{Pb}_{0.3}\text{Sr}_2\text{Ca}_2\text{Cu}_3\text{O}_x$  [10]. On the other hand, we have found that the low-resistivity part of the  $R(T)$  curves of a Bi-foamed superconductor reveal the behaviour typical for the classical flux creep model.

Figure 4 shows the Arrhenius plots ( $\log R$  versus  $1/T$ ) of resistive transitions of a Bi-foamed superconductor in different applied magnetic fields. One can see that at resistivity below  $\sim 0.1 \text{ m}\Omega \text{ cm}$  the experimental  $\log(\rho)$  versus  $(1/T)$  curves fit straight lines sufficiently well. Similar behaviour was observed in Bi single crystals [12] and polycrystalline Bi samples [10, 11]. In the classical Anderson flux creep model, the resistance caused by the motion of vortices is given by the Arrhenius relation [13]:

$$R = R_0 \exp(-U(H)/k_B T) \quad (1)$$

where  $R_0$  is the pre-exponential factor,  $U(H)$  is the activation energy. In the case of polycrystalline HTSCs,  $U(H)$  is the field dependence of an effective pinning potential in intergrain media.  $U$  values can be deduced from slopes of the  $\log R(1/T)$  curves. The inset in figure 4 shows the  $U(H)$  dependence for the studied Bi-foamed superconductor in the

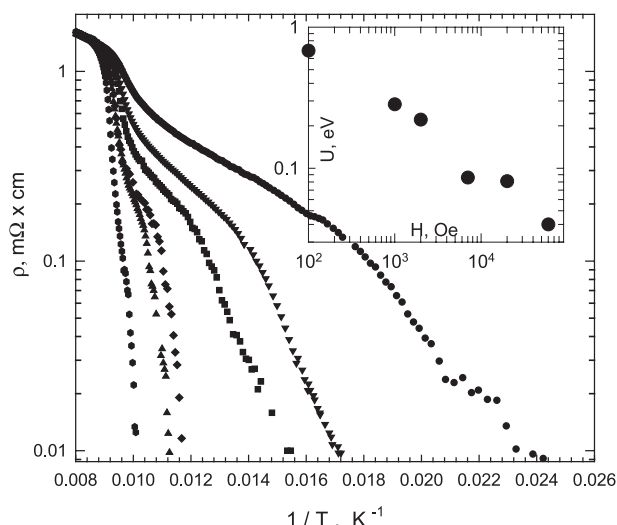


**Figure 4.** Arrhenius plots ( $\log R$  versus  $1/T$ ) of resistive transitions of the Bi-foamed superconductor in different applied magnetic fields (from left to right:  $H = 0, 0.1, 1, 2, 7, 20, 60$  kOe). Inset:  $U(H)$  dependence of BPSCCO with low density in the double logarithmic scale.

double logarithmic scale. It is seen that  $U(H)$  dependence is nearly a straight line in the double logarithmic scale, i.e.  $U(H) \sim H^{-n}$  with  $n \approx 0.45 \pm 0.02$ . This result is close to that obtained earlier in epitaxial Bi-2223 films [14–16] with  $U(H) \sim H^{-0.5}$ . The authors [15] interpreted the obtained exponent from the model of the plastic deformation of flux-line-lattice dislocations [17]. On the other hand, the exponents obtained in polycrystalline Bi-2223 [18] and silver-sheathed tapes Bi-2223 [19] differ from the value 0.5. Considering the microstructure presented in figure 1, we may assume that each microcrystallite is mechanically jointed to other crystallites only via its faces, and not via the planes as in dense polycrystals. In such a case, similarity of the physical properties of a low-density polycrystal to those of a single crystal and an epitaxial film is not surprising. The same may be said about the temperature dependence  $R(T)$  and the field dependence of activation energy  $U(H)$  observed experimentally in our samples.

Current–voltage characteristics of a Bi-foamed superconductor have been measured in the range 55–110 K. The values of critical current density have been obtained from the initial part of CVCs. Temperature dependence of the critical current density  $J_c(T)$  is plotted in figure 5. The transport critical current of granular superconductors is determined mainly by characteristics of intergrain boundaries. For this reason, in order to analyse the experimental  $J_c(T)$ , it would be reasonable to consider the theories developed for Josephson junctions. The classical de Gennes theory for superconductor (S)—normal metal (N)—superconductor (S–N–S) junctions predicts the quadratic dependence of critical current in the vicinity of the critical temperature [20]:

$$J_c \sim (1 - T/T_c)^2. \quad (2)$$

On the other hand, the Ambegaokar–Baratoff theory for S–I–S (where I is the insulator) Josephson junctions predicts linear dependence of  $J_c$  near  $T_c$ :

$$J_c \sim (1 - T/T_c). \quad (3)$$

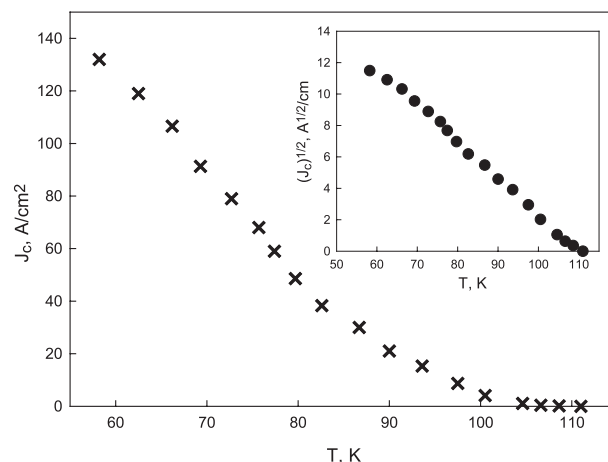


**Figure 5.** Temperature dependence of the critical current density  $J_c(T)$  of the Bi-foamed superconductor. Inset: temperature dependence of the critical current in coordinates  $J_c^{1/2}$ .

In the inset of figure 5 we have plotted an experimental temperature dependence of the critical current in coordinates  $J_c^{1/2}, T$ . It is seen that the dependence is linear. This points out the applicability of equation (2) to our experimental results. More recent theory [21] also predicts negative curvature of  $J_c(T)$  for sufficiently long S–N–S junctions. Indeed, as is seen in figure 1, the BPSCCO crystallites are jointed via cleavage areas, which play a role of metallic-type intergrain boundaries between the crystallites. The linear behaviour of  $\rho(T)$  above  $T_c$  (see figure 3) also leads to such a conclusion.

Thus, we have studied the transport properties of the novel Bi-foamed superconductor. The analysis of resistive transitions in a magnetic field has shown that the dissipation follows the thermally activated flux creep model with temperature-independent pinning potential in a network of S–N–S-type Josephson junctions.

## Acknowledgments

This work was supported by the Lavrent'evs Competition of Young Scientists of SB RAS, project N52, Integration project of SB RAS N3.4, Quantum Macrophysics Program of RAS N 3.4. KAS and DAB are grateful to the Russian Science Support Foundation.

## References

- [1] Bartolomé E *et al* 2004 *Phys. Rev. B* **70** 144514
- [2] Reddy E S and Schmitz G J 2002 *Supercond. Sci. Technol.* **15** L21
- [3] Gokhfeld D M *et al* 2006 *Physica C* **434** 135
- [4] Balaev D A *et al* 2006 *Fiz. Tverd. Tela* **48** 193 (in Russian)
- [5] Kuzmin Yu I 2003 *J. Low Temp. Phys.* **130** 261
- [6] Petrov M I *et al* 2005 *Patent Specification of Russian Federation* RU2261233
- [7] Kravchenko V S *et al* 1998 *Neorg. Mater.* **34** 1274 (in Russian)
- [8] Petrov M I *et al* 2001 *Supercond. Sci. Technol.* **14** 798
- [9] Wright A C, Zhang K and Erbil A 1991 *Phys. Rev. B* **44** 863
- [10] Bhalla G L, Malik P A and Singh K K 2003 *Physica C* **391** 17

- [11] Govea-Alcaide E *et al* 2005 *Physica C* **423** 51
- [12] Palstra T T M *et al* 1990 *Phys. Rev. B* **41** 6621
- [13] Brandt E H 1995 *Rep. Prog. Phys.* **58** 1465
- [14] Wagner P, Hillmer F, Frey U and Adrian H 1994 *Phys. Rev. B* **49** 13184
- [15] Yamasaki H *et al* 1994 *Phys. Rev. B* **49** 6913
- [16] Kucera J T, Orlando T P, Virshup G and Eckstein J N 1992 *Phys. Rev. B* **46** 11004
- [17] Geshkenbein V, Larkin A, Feigel'man M and Vinokur V 1989 *Physica C* **162–164** 239
- [18] Govea-Alcaide E *et al* 2005 *Physica C* **423** 51
- [19] Pu M H *et al* 2004 *Physica C* **412–414** 467
- [20] Barone A and Paterno J 1982 *Physics and Application of the Josephson Effect* (New York: Wiley)
- [21] Günsenheimer U, Schüssler U and Kümmel R 1994 *Phys. Rev. B* **49** 6111